

Running coupling constant of ten-flavor QCD with the Schrödinger functional method

M. Hayakawa^a, K.-I. Ishikawa^b, Y. Osaki^b, S. Takeda^c, S. Uno^a, and N. Yamada^{d,e*}

^a *Department of Physics, Nagoya University, Nagoya 464-8602, Japan*

^b *Department of Physics, Hiroshima University,*

Higashi-Hiroshima 739-8526, Japan

^c *School of Mathematics and Physics,*

College of Science and Engineering,

Kanazawa university, Kakuma-machi,

Kanazawa, Ishikawa 920-1192, Japan

^d *KEK Theory Center, Institute of Particle and Nuclear Studies,*

High Energy Accelerator Research Organization (KEK), Tsukuba 305-0801, Japan

^e *School of High Energy Accelerator Science,*

The Graduate University for Advanced Studies (Sokendai), Tsukuba 305-0801, Japan

(Dated: March 16, 2019)

Abstract

Walking technicolor theory attempts to realize electroweak symmetry breaking as the spontaneous chiral symmetry breakdown caused by the gauge dynamics with slowly varying gauge coupling constant and large mass anomalous dimension. Many-flavor QCD is one of the candidates having these features. We focus on the SU(3) gauge theory with ten massless fermions in the fundamental representation, and compute the gauge coupling constant in the Schrödinger functional scheme. Numerical simulation is performed with $O(a)$ -unimproved lattice action, and the continuum limit is taken in linear in lattice spacing. We show that this theory possesses an infrared fixed point.

*norikazu.yamada@kek.jp

I. INTRODUCTION

While the standard model has been established through a number of experiments, unnatural hierarchies are present between the electroweak scale and the Planck scale and also among the fermion masses. Large Hadron Collider (LHC) is expected to give a new insight into these hierarchies. Among various new physics models proposed so far, Technicolor (TC) model [1] is one of the most attractive ones in these regards, as it does not require any fundamental scalar particles, which cause the former hierarchy, and its extension, Extended TC model [2], has a possibility to generate the yukawa hierarchy in a dynamical way. For recent review articles, see, for example, Refs. [3].

TC should be a strongly coupled vector-like gauge system, which triggers spontaneous chiral symmetry breaking ($S\chi SB$). It is widely known, however, that the simplest TC models obtained by rescaling of ordinary QCD have already been ruled out by the S -parameter [4] and FCNC [5] constraints. Refs. [6] suggested a series of TC models to circumvent the FCNC problem. Those TC models appeal to the gauge dynamics in which the effective gauge coupling constant runs slowly (*i.e.* “walks”) at a relatively large value over a wide range of energy scale above the $S\chi SB$ scale, and in which the chiral condensate gets large anomalous dimension. Such TC is called *walking TC (WTC)*, and possible candidates have been enumerated through semi-quantitative analyses [7]. Since the dynamics that underlie WTC significantly differ from those of two or three-flavor QCD, the naive scaling argument in N_c or N_f to estimate the S -parameter would not work, and any quantitative predictions from WTC require solving nonperturbative dynamics explicitly. Lattice gauge theory provides a unique way to study this class of models from the first principles at present.

Search for candidate theories of WTC is frequently linked to the N_f -dependent phase structure of the gauge theories. Let us take $SU(3)$ gauge theory with N_f flavors of fermions in the fundamental representation as an example. According to the analysis of the perturbative β -function, the system with large enough N_f ($N_f > 16.5$) is asymptotically non-free and trivial unless non-trivial ultraviolet fixed point exists. On the other hand, if N_f is sufficiently small ($N_f \leq 3$) the dynamics is QCD-like and thus in the chirally broken phase. It is believed that for the in-between N_f there exists a so-called conformal phase, where the coupling constant reaches an infrared fixed point (IRFP) without $S\chi SB$ set in, but confinement may take place [8]. The range of N_f in which the conformal phase is realized is called conformal

window, and is represented by $N_f^{\text{crit}} < N_f < 16.5$. It is then natural to speculate that the gauge dynamics slightly below N_f^{crit} exhibit the features required for WTC; slow running of the gauge coupling constant and S χ SB. The first goal in the search for WTC is thus to identify N_f^{crit} .

In the past years, many groups have used techniques of lattice simulations to search for N_f^{crit} and/or WTC through hadron spectrum, eigenvalue distribution of Dirac operator, the behavior of running coupling constant, or renormalization group analysis of candidate theories [9]. For non-lattice studies, see, for example, Refs. [10, 11]. Among various candidates, many flavor QCD [12–18], sextet QCD [19–24], and two-color adjoint QCD [25–30] have been intensively studied. In this work, we focus on many flavor QCD with $N_c = 3$ and fermions in the fundamental representation. In a seminal work [12], the running coupling constants were calculated for eight- and twelve-flavor QCD using the Schrödinger functional (SF) scheme on the lattice [31]. They concluded that twelve-flavor QCD has an IRFP at $g_{\text{SF}}^2 \sim 5$ while eight-flavor QCD does not. In principle, the study of the running coupling alone is not supposed to be able to fully exclude the possibility of a large IRFP because the unphysical, bulk first-order phase transition [22, 32, 33] prevents one from studying the running at arbitrarily large values of the renormalized coupling constant. Nevertheless, because of the supports from the spectroscopy studies [13, 15, 17] the conclusion in Ref. [12] that the eight-flavor QCD is QCD-like, *i.e.* $N_f^{\text{crit}} > 8$, seems to be well established nowadays.

After the work of Ref. [12], one group [14] has presented an evidence of the conformality of twelve-flavor QCD. The opposite conclusion, however, has also been reported by the other groups [15, 17]. Therefore $N_f^{\text{crit}} < 12$ is still under debate. Clearly the observed contradiction must be clarified before going further. While in the spectroscopy study of twelve-flavor QCD many sources of systematic uncertainties due to finite volume, taste breaking, chiral extrapolation, lack of continuum limit, *etc.*, remain to be quantified, it appears, at least, to us that there is no reason to doubt the existence of IRFP in the study of the SF coupling constant. In such a circumstance, we are tempted to explore the dynamics of ten-flavor QCD. In this paper, we investigate the running coupling constant of ten-flavor QCD from the lattice simulation as the first step.

The paper is organized as follows. Sec. II summarizes the coefficients relevant to the perturbative calculation of the running coupling constant for later use. In sec. III, the simulation setup including the definition of the running coupling constant in the Schrödinger

functional scheme is presented. In sec. IV, we explain the analysis method and present the numerical results. Sec. V is devoted to the summary and outlook.

II. PERTURBATIVE ANALYSIS

We start with defining the β function of an effective gauge coupling constant in a mass-independent renormalization scheme, which should have the following expansion in the perturbative regime

$$\beta(g^2(L)) = L \frac{\partial g^2(L)}{\partial L} = b_1 g^4(L) + b_2 g^6(L) + b_3 g^8(L) + b_4 g^{10}(L) + \dots, \quad (1)$$

where L denotes a length scale. The first two coefficients on the right hand side are scheme-independent, and given by

$$b_1 = \frac{2}{(4\pi)^2} \left[11 - \frac{2}{3} N_f \right], \quad b_2 = \frac{2}{(4\pi)^4} \left[102 - \frac{38}{3} N_f \right]. \quad (2)$$

The remaining coefficients are scheme-dependent and known only in the limited schemes and orders. The third coefficient takes the following form in the Schrödinger functional scheme;

$$b_3^{\text{SF}} = b_3^{\overline{\text{MS}}} + \frac{b_2 c_2^\theta}{2\pi} - \frac{b_1 (c_3^\theta - c_2^{\theta^2})}{8\pi^2}, \quad (3)$$

where $b_3^{\overline{\text{MS}}}$ is a coefficient in the $\overline{\text{MS}}$ scheme,

$$b_3^{\overline{\text{MS}}} = \frac{2}{(4\pi)^6} \left[\frac{2857}{2} - \frac{5033}{18} N_f + \frac{325}{54} N_f^2 \right], \quad (4)$$

and the calculable quantities c_2^θ and c_3^θ depend on the spatial boundary condition imposed on the fermion fields in the SF setup, *i.e* so-called θ . Those for $\theta = \pi/5$ and c_2^θ for $\theta = 0$ are known to be [34]

$$c_2^{\theta=\pi/5} = 1.25563 + 0.039863 \times N_f, \quad (5)$$

$$c_3^{\theta=\pi/5} = (c_2^{\theta=\pi/5})^2 + 1.197(10) + 0.140(6) \times N_f - 0.0330(2) \times N_f^2, \quad (6)$$

$$c_2^{\theta=0} = 1.25563 + 0.022504 \times N_f, \quad (7)$$

but $c_3^{\theta=0}$ has not been calculated yet. Although $\theta = 0$ is chosen in our simulation as described in sec. III, the coefficients for $\theta = \pi/5$ are used only to see the situation of conformal windows inferred just from the perturbative analysis, and the potential size of difference between the two- and three-loop calculations.

N_f	4	6	8	10	12	14	16
two-loop universal	-	-	-	27.74	9.47	3.49	0.52
three-loop SF with $\theta = \pi/5$	43.36	23.75	15.52	9.45	5.18	2.43	0.47

TABLE I: The perturbative IRFP obtained from the two-loop universal and the three-loop SF scheme analyses.

The perturbative estimates of the infrared fixed point (IRFP) for SU(3) gauge theory with N_f flavors of fundamental fermion are summarized in Tab. I. We note that in the three-loop perturbative analysis the existence of IRFP is determined only by the sign of $c_3^{\theta=\pi/5}$, which is always negative for the range of N_f shown in Tab. I. Therefore, the existence of IRFP as well as its value may be unstable against including higher orders. Nevertheless, for $N_f \geq 14$ the difference between the two- and three-loop results is reasonably small, and one may expect that higher order corrections do not spoil the existence of IRFP or even do not change its value by much for such a large N_f .

According to the analysis based on Schwinger-Dyson equation, S χ SB is expected to occur when the running coupling constant reaches $g^2 \sim \pi^2$ in SU(3) gauge theories [35]. In spite of the scheme-dependence of the running coupling constant and the value of IRFP, those results motivate us to speculate that ten-flavor QCD may exhibit strongly coupled walking dynamics, and thus deserves full nonperturbative calculation.

III. SIMULATION DETAILS

A. Schrödinger functional

We employ the Schrödinger functional (SF) method [31] to study the scale dependence of the running coupling constant. Unimproved Wilson fermion action and the standard plaquette gauge action are used without any boundary counter terms as described below.

The SF on the lattice is defined on a four dimensional hypercubic lattice with a volume $(L/a)^3 \times (T/a)$ in the cylindrical geometry. Throughout this work, the temporal extent T/a is chosen to be equal to the spatial one L/a . Periodic boundary condition in the spatial directions with vanishing phase factor ($\theta = 0$) and Dirichlet one in the temporal direction are imposed for both gauge ($U_\mu(x)$) and fermion ($\psi(x)$ and $\bar{\psi}(x)$) fields. The boundary

values for gauge and fermion fields are represented by three-by-three color matrices, C and C' , and spinors, ρ , ρ' , $\bar{\rho}$ and $\bar{\rho}'$, respectively. The partition function of this system is given by

$$Z_{\text{SF}}(C', \bar{\rho}', \rho'; C, \bar{\rho}, \rho) = e^{-\Gamma(C', \bar{\rho}', \rho'; C, \bar{\rho}, \rho)} = \int D[U, \psi, \bar{\psi}] e^{-S[U, \psi, \bar{\psi}, C, C', \rho, \rho', \bar{\rho}, \bar{\rho}']}, \quad (8)$$

where Γ is the effective action, and

$$S[U, \psi, \bar{\psi}, C, C', \rho, \rho', \bar{\rho}, \bar{\rho}'] = S_g[U, C, C'] + S_q[U, \psi, \bar{\psi}, \rho, \rho', \bar{\rho}, \bar{\rho}']. \quad (9)$$

For the pure gauge part, we employ the plaquette action,

$$S_g[U, C, C'] = \frac{\beta}{6} \sum_x \sum_{\mu=0}^3 \sum_{\nu=0}^3 \bar{\delta}_{\mu,\nu} w_{\mu,\nu}(x_0) \text{Tr} [1 - P_{\mu,\nu}(x)], \quad (10)$$

where $\beta = 6/g_0^2$ denotes the inverse of the bare coupling constant, $\bar{\delta}_{\mu,\nu}=0$ when $\mu = \nu$ otherwise 1, and $P_{\mu,\nu}(x)$ denotes a 1×1 Wilson loop on the μ - ν plane starting and ending at x . The spatial link variables on the boundaries, the hypersurfaces at $x_0 = 0$ and L/a , are all set to the diagonal, constant $SU(3)$ matrices as

$$U_k(x)|_{x_0=0} = \exp[C], \quad C = \frac{ia}{L} \begin{pmatrix} \eta - \frac{\pi}{3} & 0 & 0 \\ 0 & -\frac{1}{2}\eta & 0 \\ 0 & 0 & -\frac{1}{2}\eta + \frac{\pi}{3} \end{pmatrix}, \quad (11)$$

$$U_k(x)|_{x_0=L/a} = \exp[C'], \quad C' = \frac{ia}{L} \begin{pmatrix} -\eta - \pi & 0 & 0 \\ 0 & \frac{1}{2}\eta + \frac{\pi}{3} & 0 \\ 0 & 0 & \frac{1}{2}\eta + \frac{2\pi}{3} \end{pmatrix}, \quad (12)$$

where $k = 1, 2, 3$, and η is parameterizing the gauge boundary fields. The weight $w_{\mu,\nu}(x_0)$ in eq. (10) is given by

$$w_{\mu,\nu}(x_0) = \begin{cases} c_t & \text{for } (t = 0 \text{ or } t = (L/a) - 1) \text{ and } (\mu \text{ or } \nu=0) \\ 0 & \text{for } (t = (L/a)) \text{ and } (\mu \text{ or } \nu=0) \\ \frac{1}{2}c_s & \text{for } (t = 0 \text{ or } t = (L/a)) \text{ and } (\mu \neq 0 \text{ and } \nu \neq 0) \\ 1 & \text{for all the other cases} \end{cases}. \quad (13)$$

By tuning c_t , $O(a)$ errors induced from the boundaries in the time direction can be removed perturbatively, but in this work we simply take its tree level values, $c_t = 1$. With this setup,

the value of c_s can be arbitrarily chosen because the spatial plaquettes on the boundaries do not contribute to the action. We thus set $c_s = 0$.

The fermion fields are described by the unimproved Wilson fermion action,

$$S_q[U, \psi, \bar{\psi}] = N_f \sum_{x,y} \bar{\psi}(x) D(x, y; U) \psi(y) = N_f \sum_{x,y} \bar{\psi}^{\text{lat}}(x) D^{\text{lat}}(x, y; U) \psi^{\text{lat}}(y), \quad (14)$$

$$D^{\text{lat}}(x, y; U) = \delta_{xy} - \kappa \sum_{\mu} \{ (1 - \gamma_{\mu}) U_{\mu}(x) \delta_{x+\hat{\mu}, y} + (1 + \gamma_{\mu}) U_{\mu}^{\dagger}(x - \hat{\mu}) \delta_{x-\hat{\mu}, y} \}, \quad (15)$$

where

$$\psi^{\text{lat}}(x) = \frac{1}{\sqrt{2\kappa}} \psi(x), \quad \bar{\psi}^{\text{lat}}(x) = \frac{1}{\sqrt{2\kappa}} \bar{\psi}(x), \quad D^{\text{lat}}(x, y; U) = 2\kappa D(x, y; U). \quad (16)$$

The hopping parameter κ is related to the bare mass m_0 through $2\kappa = 1/(am_0 + 4)$. The dynamical degrees of freedom of the fermion field $\psi(x)$ and anti-fermion fields $\bar{\psi}(x)$ reside on the lattice sites x with $0 < x_0 < T$. On both boundaries ($x_0 = 0$ and T), the half of the Dirac components are set to zero and the remaining components are fixed to some prescribed values, ρ , $\bar{\rho}$, ρ' and $\bar{\rho}'$, as

$$P_+ \psi(x)|_{x_0=0} = \rho(\mathbf{x}), \quad P_- \psi(x)|_{x_0=0} = 0, \quad (17)$$

$$P_- \psi(x)|_{x_0=T} = \rho'(\mathbf{x}), \quad P_+ \psi(x)|_{x_0=T} = 0, \quad (18)$$

$$\bar{\psi}(x) P_- |_{x_0=0} = \bar{\rho}(\mathbf{x}), \quad \bar{\psi}(x) P_+ |_{x_0=0} = 0, \quad (19)$$

$$\bar{\psi}(x) P_+ |_{x_0=T} = \bar{\rho}'(\mathbf{x}), \quad \bar{\psi}(x) P_- |_{x_0=T} = 0, \quad (20)$$

where $P_{\pm} = (1 \pm \gamma_0)/2$. In this work, the boundary values for the fermion fields are set to zero, *i.e.*

$$\rho = \rho' = \bar{\rho} = \bar{\rho}' = 0. \quad (21)$$

B. Definition of the running coupling

With the gauge boundary conditions (11) and (12), the absolute minimum of the action is given by a color-electric background field denoted by $B(x)$. Then, the effective action can be defined as a function of B by

$$\Gamma[B] = -\ln Z_{\text{SF}}(C', \bar{\rho}', \rho'; C, \bar{\rho}, \rho), \quad (22)$$

which has the following perturbative expansion in the bare coupling constant,

$$\Gamma = \frac{1}{g_0^2} \Gamma_0 + \Gamma_1 + O(g_0^2), \quad (23)$$

and, in particular, the lowest-order term

$$\Gamma_0 = [g_0^2 S_g[B]]_{g_0=0}, \quad (24)$$

is exactly the classical action of the induced background field. The SF scheme coupling is then defined in the massless limit for fermions by

$$\left. \frac{\partial \Gamma}{\partial \eta} \right|_{\eta=0} = \frac{1}{g_{\text{SF}}^2(g_0^2, l = L/a)} \left. \frac{\partial \Gamma_0}{\partial \eta} \right|_{\eta=0} = \frac{k}{g_{\text{SF}}^2(g_0^2, l)}, \quad (25)$$

where the normalization constant k is determined such that $g_{\text{SF}}^2 = g_0^2$ holds in the leading order of the perturbative expansion, and is found to be

$$k = \left. \frac{\partial \Gamma_0}{\partial \eta} \right|_{\eta=0} = 12 \left(\frac{L}{a} \right)^2 [\sin(2\gamma) + \sin(\gamma)] = k \quad \text{with } \gamma = \frac{\pi}{3} \left(\frac{a}{L} \right)^2. \quad (26)$$

Because of the absence of the clover term, only the η -derivative of the gauge action contributes to $1/g_{\text{SF}}^2(g_0^2, l)$.

C. Parameters

The simulation was performed on the lattice sizes of $l^4 = (L/a)^4 = 4^4, 6^4, 8^4, 12^4$, and 16^4 with the inverse of bare gauge coupling constant $\beta = 6/g_0^2$ in the range, $4.4 \leq \beta \leq 96.0$. However, the data from $l = 4$ lattices are not used in the following analysis because it was found that they have large discretization errors. We calculated the SF coupling on 18^4 lattice with a single β ($\beta=4.55$), and the result is used to check the scaling violation at a specific value of g_{SF}^2 .

The algorithm to generate the gauge configuration follows the standard HMC with five pseudo-fermion fields introduced to simulate the ten flavors of dynamical fermions. The numerical simulations were carried out on several different architectures including GPGPU, PC cluster and supercomputers. In order to achieve high performance on each architecture, the HMC code, especially the fermion solver part, were optimized depending on each architecture. In particular, mixed precision solver using multiple GPUs enables us to obtain

high statistics on g_{SF}^2 at $l^4 = 12^4$ and 16^4 [36]. Acceptance ratio is kept to around 80 % by adjusting the molecular dynamics step size ($\delta\tau$).

Since the Wilson fermion explicitly breaks chiral symmetry, the value of κ is tuned, for every pair of $(\beta, L/a)$, to its critical value κ_c realizing the massless fermion by monitoring the corresponding PCAC mass. The values of β , κ , the number of trajectories, $\delta\tau$ and the results for $l = L/a=6, 8, 12, 16$, and 18 lattices are tabulated in Tabs. II-VI, respectively.

D. Comment on $O(a)$ -unimprovement

In our pilot study, we employed the $O(a)$ -improved fermion action with the perturbatively determined counter terms. With this setup, we encountered a sudden change of the plaquette and the PCAC mass at $l=6$ and $\beta=3.6$ when κ was decreased from 0.1517, and we could not realize the vanishing PCAC mass. The expected SF coupling constant is about $3 \sim 4$ there. The same phenomenon also occurs on $l = 4$ lattices at almost the same value of bare coupling constant. Since the observed behavior looks similar to those reported in Refs. [22, 32, 33], we infer that this is a bulk, first order phase transition. In order to cover the region $g_{\text{SF}}^2 \sim O(10)$, we omitted any $O(a)$ improvements. Thus the leading discretization error in our result is linear in lattice spacing.

Even without $O(a)$ improvements, the bulk, first order phase transition is observed for $\beta = 6/g_0^2 \sim 4.4$. However, this time it happens at the renormalized coupling constant greater than the $O(a)$ -improved case, typically $g_{\text{SF}}^2 \sim O(10)$. Since this bulk phase transition is considered as a lattice artifact, whenever this happens we discard the gauge configurations at such β . Thus the position of the critical β (~ 4.4) sets the lower limit on our exploration of β .

IV. ANALYSIS METHOD AND RESULTS

A. Raw data

The SF coupling constant (g_{SF}^2) and the PCAC mass (M) obtained on each (β, κ, l) are shown in Tabs. II-VI. g_0^2/g_{SF}^2 is plotted as a function of the bare coupling constant g_0^2 in Fig. 1. The figure shows that g_{SF}^2 increases with $l = L/a$ at a fixed g_0^2 , but the change between the data from $l = 12$ and $l = 16$ is tiny. For later use, we fit the data of g_0^2/g_{SF}^2

to an interpolating formula as a function of the bare coupling constant g_0^2 . Among various functional forms we examined, the following form

$$\frac{g_0^2}{g_{\text{SF}}^2(g_0^2, l)} = \frac{1 - a_{l,1} g_0^4}{1 + p_{1,l} \times g_0^2 + \sum_{n=2}^N a_{l,n} \times g_0^{2n}}, \quad (27)$$

turned out to give the minimum χ^2/dof for a fixed number of free parameters, N . We thus employ eq. (27). In eq. (27), $p_{1,l}$ is the l -dependent coefficient and we have calculated them perturbatively in the SF scheme

$$p_{1,l} = \begin{cases} 0.4477107831 & \text{for } l = 6 \\ 0.4624813408 & \text{for } l = 8 \\ 0.4756888260 & \text{for } l = 12 \\ 0.4833079203 & \text{for } l = 16 \\ 0.4864767958 & \text{for } l = 18 \end{cases} . \quad (28)$$

The other coefficients $a_{l,n}$'s are determined for each l independently. We optimize the degree of polynomial N in the denominator of eq. (27) by monitoring χ^2/dof , and take $N = 5$ for $l = 6$ and 12, and $N = 4$ for $l = 8$ and 16. Tab. VII shows the fit results for the coefficients in eq. (27). The fit results are also shown as the region sandwiched by a pair of solid curves in Fig. 1.

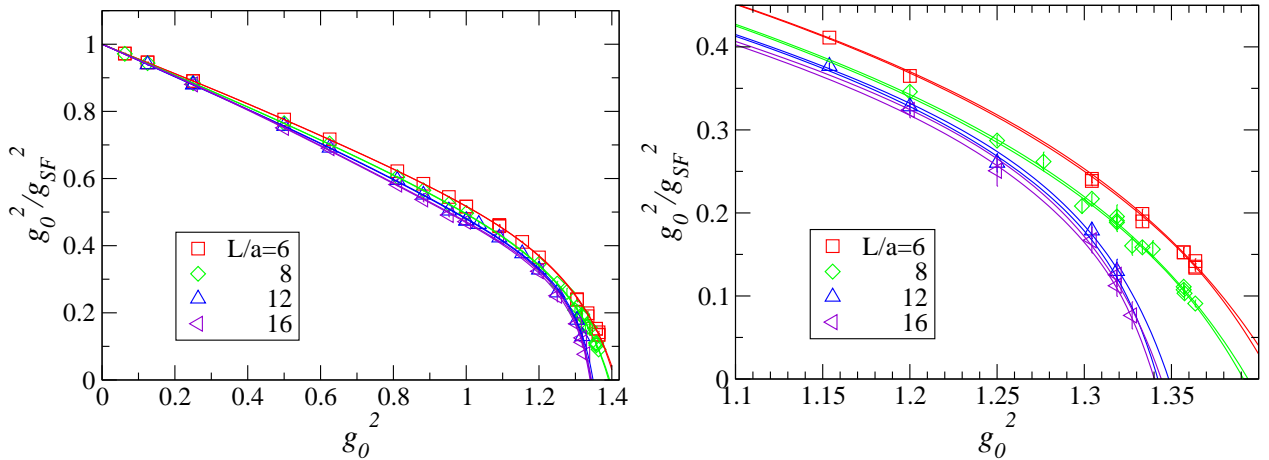


FIG. 1: g_0^2 dependence of g_0^2/g_{SF}^2 for $l = L/a=6, 8, 12$ and 16. The right panel magnifies the region of $g_0^2 \in [1.1, 1.40]$.

Hereafter we denote the SF coupling obtained at a bare coupling constant g_0^2 and at a lattice length of l by $g_{\text{SF}}^2(g_0^2, l)$ and its continuum counterpart by $g_{\text{SF}}^2(L)$.

β	κ	Trajs.	plq.	$\delta\tau$	Acc.	g_{SF}^2	M
96.0000	0.1267030	39,700	0.979268(0.000002)	0.0076	0.827(0.002)	0.06431(0.00006)	0.00012(0.00003)
96.0000	0.1267070	49,900	0.979267(0.000002)	0.0076	0.826(0.002)	0.06428(0.00005)	-0.00004(0.00003)
48.0000	0.1276060	40,100	0.958852(0.000005)	0.0098	0.857(0.002)	0.13221(0.00010)	-0.00013(0.00002)
48.0000	0.1276100	41,100	0.958846(0.000004)	0.0098	0.857(0.002)	0.13209(0.00010)	-0.00016(0.00002)
24.0000	0.1295180	24,700	0.917566(0.000009)	0.0149	0.848(0.002)	0.28079(0.00015)	0.00006(0.00002)
24.0000	0.1295200	60,300	0.917562(0.000005)	0.0152	0.838(0.002)	0.28086(0.00010)	0.00006(0.00001)
12.0000	0.1339640	48,700	0.833056(0.000014)	0.0250	0.812(0.002)	0.64450(0.00076)	-0.00004(0.00005)
9.6000	0.1365680	160,300	0.789765(0.000012)	0.0256	0.826(0.001)	0.87189(0.00068)	0.00002(0.00003)
7.4000	0.1410690	120,500	0.724148(0.000015)	0.0270	0.854(0.001)	1.30413(0.00194)	0.00006(0.00006)
6.8000	0.1430520	120,300	0.698517(0.000018)	0.0270	0.870(0.001)	1.51024(0.00244)	-0.00025(0.00008)
6.3000	0.1451400	17,400	0.673231(0.000076)	0.0333	0.817(0.001)	1.74788(0.00505)	0.00015(0.00019)
6.0000	0.1466380	33,600	0.655993(0.000034)	0.0333	0.837(0.002)	1.93684(0.00691)	0.00044(0.00021)
6.0000	0.1466410	80,300	0.655981(0.000029)	0.0333	0.833(0.001)	1.93605(0.00362)	0.00004(0.00010)
5.5000	0.1497590	50,300	0.622923(0.000025)	0.0370	0.817(0.002)	2.38340(0.01092)	0.00042(0.00020)
5.5000	0.1497610	36,000	0.622942(0.000027)	0.0357	0.827(0.002)	2.36232(0.00634)	-0.00018(0.00022)
5.5000	0.1497620	140,300	0.622977(0.000023)	0.0357	0.831(0.001)	2.37542(0.00963)	0.00023(0.00014)
5.2000	0.1521330	220,300	0.600097(0.000019)	0.0380	0.812(0.001)	2.80668(0.01246)	-0.00015(0.00014)
5.0000	0.1539800	59,900	0.583463(0.000049)	0.0400	0.806(0.002)	3.28837(0.06618)	-0.00005(0.00046)
4.6000	0.1585140	33,800	0.545776(0.000055)	0.0400	0.813(0.002)	5.47008(0.13064)	0.00092(0.00043)
4.6000	0.1585150	150,000	0.545680(0.000041)	0.0400	0.813(0.001)	5.41263(0.09891)	0.00123(0.00042)
4.5000	0.1599020	100,300	0.535280(0.000061)	0.0400	0.813(0.001)	7.02516(0.24479)	0.00111(0.00069)
4.5000	0.1599030	100,300	0.535305(0.000066)	0.0400	0.813(0.002)	6.70575(0.19622)	0.00033(0.00061)
4.4215	0.1610680	105,900	0.526537(0.000087)	0.0385	0.825(0.001)	8.88882(0.36944)	0.00238(0.00097)
4.4215	0.1610820	92,400	0.526692(0.000066)	0.0385	0.826(0.001)	8.90139(0.32355)	0.00073(0.00075)
4.4000	0.1614210	249,500	0.524331(0.000060)	0.0400	0.811(0.001)	9.60163(0.19661)	0.00051(0.00050)
4.4000	0.1614220	182,500	0.524342(0.000091)	0.0400	0.812(0.001)	10.17980(0.33990)	0.00119(0.00073)
4.4000	0.1614230	250,500	0.524387(0.000062)	0.0400	0.811(0.001)	10.07713(0.25379)	0.00049(0.00053)

TABLE II: Simulation parameters and results obtained at $L/a=6$.

β	κ	Trajs.	plq.	$\delta\tau$	Acc.	g_{SF}^2	M
96.0000	0.1263270	22,500	0.979420(0.000002)	0.0056	0.811(0.004)	0.06434(0.00004)	0.00001(0.00001)
48.0000	0.1272250	18,300	0.958843(0.000003)	0.0100	0.818(0.007)	0.13247(0.00017)	0.00002(0.00002)
24.0000	0.1291450	42,300	0.917260(0.000004)	0.0125	0.804(0.003)	0.28282(0.00023)	-0.00004(0.00002)
12.0000	0.1335850	68,500	0.832266(0.000007)	0.0167	0.828(0.005)	0.65380(0.00071)	-0.00010(0.00003)
9.6000	0.1361800	21,820	0.788830(0.000013)	0.0200	0.828(0.006)	0.88751(0.00287)	-0.00008(0.00005)
7.4000	0.1406600	63,330	0.723081(0.000010)	0.0250	0.818(0.003)	1.34182(0.00417)	-0.00004(0.00016)
6.8000	0.1426200	41,500	0.697409(0.000013)	0.0250	0.797(0.002)	1.56232(0.00662)	0.00012(0.00011)
6.3000	0.1447000	28,000	0.672208(0.000021)	0.0250	0.816(0.003)	1.81987(0.01036)	-0.00034(0.00014)
6.0000	0.1462000	47,000	0.654999(0.000012)	0.0250	0.820(0.003)	2.01248(0.01258)	-0.00042(0.00011)
5.0000	0.1533600	27,900	0.582458(0.000038)	0.0250	0.825(0.004)	3.46930(0.07238)	0.00094(0.00034)
4.8000	0.1554270	114,500	0.564464(0.000020)	0.0250	0.860(0.001)	4.35348(0.09845)	0.00026(0.00024)
4.7000	0.1565500	35,400	0.554789(0.000040)	0.0256	0.854(0.002)	4.87595(0.21035)	0.00027(0.00051)
4.6200	0.1575500	86,300	0.546856(0.000030)	0.0312	0.783(0.001)	6.23744(0.25321)	-0.00023(0.00033)
4.6000	0.1577800	149,300	0.544695(0.000027)	0.0250	0.852(0.002)	6.01108(0.17093)	-0.00007(0.00028)
4.5500	0.1584200	24,500	0.539428(0.000090)	0.0278	0.833(0.003)	6.92022(0.46491)	0.00087(0.00088)
4.5500	0.1584270	93,300	0.539336(0.000033)	0.0278	0.831(0.002)	6.99432(0.31873)	0.00135(0.00041)
4.5500	0.1584500	25,700	0.539683(0.000064)	0.0278	0.832(0.004)	6.74187(0.46970)	-0.00163(0.00071)
4.5200	0.1588500	56,570	0.536316(0.000058)	0.0278	0.827(0.002)	8.28029(0.57687)	-0.00010(0.00059)
4.5000	0.1591300	107,100	0.534108(0.000036)	0.0250	0.859(0.001)	8.40630(0.37369)	-0.00007(0.00038)
4.4800	0.1594000	41,555	0.531781(0.000085)	0.0250	0.827(0.002)	8.57214(0.57202)	0.00027(0.00070)
4.4215	0.1602640	160,900	0.525143(0.000050)	0.0263	0.837(0.001)	12.21877(0.49625)	-0.00012(0.00041)
4.4215	0.1602700	127,500	0.525149(0.000058)	0.0250	0.861(0.001)	12.62365(0.68980)	-0.00059(0.00048)
4.4200	0.1602700	29,700	0.524651(0.000132)	0.0278	0.828(0.002)	13.15085(0.99774)	0.00214(0.00075)
4.4000	0.1606000	229,500	0.522502(0.000057)	0.0278	0.819(0.002)	15.00764(0.69115)	0.00020(0.00042)

TABLE III: Simulation parameters and results obtained at $L/a=8$.

B. Discrete β function

In order to see the scale dependence of the SF coupling constant, we analyze the discrete β function (DBF) introduced in Refs. [19, 22]. The whole procedure is described below.

β	κ	Trajs.	plq.	$\delta\tau$	Acc.	g_{SF}^2	M
48.0000	0.1269700	11,200	0.958648(0.000002)	0.0056	0.815(0.003)	0.13304(0.00033)	-0.00014(0.00003)
24.0000	0.1288891	6,100	0.916772(0.000004)	0.0083	0.804(0.002)	0.28395(0.00077)	-0.00004(0.00003)
24.0000	0.1288929	41,940	0.916777(0.000002)	0.0083	0.799(0.003)	0.28428(0.00037)	-0.00010(0.00001)
12.0000	0.1333359	53,355	0.831307(0.000003)	0.0125	0.807(0.003)	0.66114(0.00103)	-0.00006(0.00002)
9.6000	0.1359350	64,200	0.787679(0.000003)	0.0133	0.805(0.002)	0.90400(0.00246)	-0.00002(0.00003)
7.4000	0.1404060	57,850	0.721829(0.000006)	0.0154	0.803(0.003)	1.36220(0.00664)	-0.00007(0.00006)
6.8000	0.1423250	45,150	0.696157(0.000006)	0.0167	0.819(0.002)	1.59998(0.00983)	0.00091(0.00006)
6.3000	0.1444050	23,500	0.671015(0.000014)	0.0182	0.767(0.002)	1.89012(0.01692)	0.00013(0.00012)
6.0000	0.1459000	20,760	0.653903(0.000009)	0.0182	0.788(0.003)	2.10541(0.02351)	0.00025(0.00007)
6.0000	0.1459000	22,536	0.653899(0.000012)	0.0154	0.848(0.001)	2.11064(0.03591)	0.00001(0.00010)
5.8000	0.1470200	36,200	0.641480(0.000008)	0.0182	0.800(0.002)	2.22863(0.02673)	-0.00006(0.00008)
5.5000	0.1489400	31,500	0.621183(0.000010)	0.0167	0.834(0.003)	2.57395(0.02665)	-0.00024(0.00009)
5.2000	0.1512000	68,000	0.598557(0.000009)	0.0200	0.781(0.002)	3.06212(0.03210)	0.00056(0.00009)
5.0000	0.1529700	64,341	0.582083(0.000009)	0.0167	0.825(0.002)	3.65676(0.09087)	0.00001(0.00012)
4.8000	0.1549700	64,500	0.564212(0.000011)	0.0182	0.798(0.004)	4.80315(0.20073)	0.00016(0.00018)
4.6000	0.1572300	127,922	0.544423(0.000012)	0.0182	0.818(0.002)	7.29885(0.38589)	0.00075(0.00017)
4.5500	0.1578500	57,260	0.539025(0.000021)	0.0192	0.802(0.002)	10.15231(1.11827)	0.00125(0.00027)

TABLE IV: Simulation parameters and results obtained at $L/a=12$.

First, we choose an initial value of the running coupling constant, denoted by u . This implicitly sets the initial length scale L_0 through $g_{\text{SF}}^2(L_0) = u$. Using the interpolating formula (27) for the lattice size l ($= L/a$), the bare coupling constant g_0^* is numerically obtained by solving the equation $g_{\text{SF}}^2(g_0^{*2}, l) = u$. l is identified with L_0/a , so that the lattice spacing at g_0^{*2} is found to be $a(g_0^{*2}, l) = L_0/l$. Now we choose a step scaling factor (length rescaling parameter), s . The lattice step scaling function $\Sigma_0(u, s, l)$ is then defined as the SF coupling for $l' = s \cdot l$ at the same bare coupling g_0^{*2} , *i.e.*

$$\Sigma_0(u, s, l) \equiv g_{\text{SF}}^2(g_0^{*2}, s \cdot l) \Big|_{g_{\text{SF}}^2(g_0^{*2}, l)=u}. \quad (29)$$

The meaning of the subscript “0” becomes clear soon. Of course, both l and $s \cdot l$ must be equal to one of 6, 8, 12 and 16, and hence the possible values for the step scaling factor s

β	κ	Trajs.	plq.	$\delta\tau$	Acc.	g_{SF}^2	M
24.0000	0.1288000	21,330	0.916504(0.000002)	0.0067	0.797(0.003)	0.28393(0.00058)	0.00011(0.00001)
12.0000	0.1332590	22,900	0.830796(0.000005)	0.0091	0.668(0.011)	0.66587(0.00413)	-0.00017(0.00003)
9.6000	0.1358600	30,900	0.787096(0.000002)	0.0080	0.807(0.003)	0.90538(0.00570)	-0.00023(0.00003)
7.4000	0.1403250	42,580	0.721189(0.000004)	0.0111	0.814(0.002)	1.39352(0.00859)	0.00002(0.00005)
6.8000	0.1422900	27,576	0.695617(0.000004)	0.0133	0.790(0.002)	1.64125(0.02186)	-0.00041(0.00006)
6.3000	0.1443400	45,640	0.670502(0.000005)	0.0133	0.799(0.003)	1.93843(0.02107)	-0.00034(0.00005)
6.0000	0.1457950	18,900	0.653363(0.000007)	0.0156	0.712(0.004)	2.12147(0.03887)	0.00043(0.00010)
5.5000	0.1488500	18,800	0.620886(0.000009)	0.0143	0.788(0.004)	2.55876(0.05312)	-0.00023(0.00010)
5.0000	0.1528550	36,949	0.582113(0.000005)	0.0143	0.799(0.002)	3.70466(0.10637)	-0.00009(0.00012)
4.8000	0.1548310	28,200	0.564443(0.000008)	0.0156	0.756(0.003)	4.98699(0.36176)	-0.00016(0.00013)
4.6000	0.1570500	51,362	0.544762(0.000012)	0.0143	0.794(0.002)	7.80446(0.71853)	0.00122(0.00016)
4.5500	0.1576750	54,922	0.539588(0.000012)	0.0139	0.819(0.002)	11.73861(1.33120)	0.00033(0.00016)
4.5500	0.1576800	43,987	0.539631(0.000018)	0.0143	0.794(0.002)	10.51607(1.16044)	-0.00008(0.00017)
4.5200	0.1580650	42,400	0.536387(0.000021)	0.0156	0.754(0.002)	17.34193(3.72829)	-0.00030(0.00021)

TABLE V: Simulation parameters and results obtained at $L/a=16$.

β	κ	Trajs.	plq.	$\delta\tau$	Acc.	g_{SF}^2	M
4.5500	0.1576500	21,334	0.540097(0.000018)	0.0143	0.780(0.005)	9.97122(1.16952)	-0.00120(0.00019)

TABLE VI: Simulation parameters and results obtained at $L/a=18$.

are limited. The difference between $\Sigma_0(u, s, l)$ and u gives the scale dependence through the scale change from L to $s \cdot L$, up to lattice artifacts.

Since the raw data of $1/g_{\text{SF}}^2(g_0^2, l)$ fluctuate around zero in the strong coupling region, converting from $1/g_{\text{SF}}^2(g_0^2, l)$ to $g_{\text{SF}}^2(g_0^2, l)$ sometimes induces huge statistical uncertainty. To avoid this we treat the inverse coupling constant, $1/g_{\text{SF}}^2(g_0^2, l)$, directly. Then, to see the scale dependence of the inverse coupling constant, we introduce the lattice DBF [19, 22] by

$$B_0(u, s, l) = \frac{1}{\Sigma_0(u, s, l)} - \frac{1}{u}. \quad (30)$$

We calculate the continuum limit of this function for various initial values of the coupling constant, u . If the sign of the DBF in the continuum limit turns out to flip at a certain

L/a	N	χ^2/dof	$a_{L/a,1}$	$a_{L/a,2}$	$a_{L/a,3}$	$a_{L/a,4}$	$a_{L/a,5}$
6	3	9.0(1.3)	0.4906(0.0025)	-0.2749(0.0105)	-0.1897(0.0151)		
6	4	1.4(0.5)	0.5048(0.0014)	-0.3993(0.0119)	0.1136(0.0283)	-0.2042(0.0184)	
6	5	1.3(0.5)	0.5015(0.0032)	-0.4240(0.0256)	0.2538(0.1301)	-0.4043(0.1815)	0.0899(0.0808)
8	3	2.0(0.6)	0.5057(0.0019)	-0.2352(0.0105)	-0.2314(0.0157)		
8	4	0.5(0.3)	0.5147(0.0020)	-0.3418(0.0264)	0.0423(0.0647)	-0.1832(0.0408)	
8	5	0.5(0.6)	0.5152(0.0043)	-0.3255(0.1478)	-0.0331(0.6572)	-0.0835(0.8533)	-0.0410(0.3452)
12	3	2.5(0.9)	0.5160(0.0068)	-0.1949(0.0109)	-0.2817(0.0221)		
12	4	1.0(0.6)	0.5416(0.0062)	-0.3591(0.0418)	0.1056(0.0987)	-0.2732(0.0655)	
12	5	0.8(0.5)	0.5500(0.0065)	-0.2658(0.0734)	-0.3588(0.3168)	0.3632(0.4140)	-0.2790(0.1764)
16	3	3.5(1.2)	0.5315(0.0061)	-0.1824(0.0307)	-0.3095(0.0448)		
16	4	0.9(0.6)	0.5535(0.0039)	-0.4833(0.0607)	0.4323(0.1370)	-0.4848(0.0822)	
16	5	0.9(0.6)	0.5563(0.0046)	-0.3995(0.1270)	0.0191(0.5528)	0.0825(0.7310)	-0.2398(0.3040)

TABLE VII: The results for the coefficients in the fit function (27)

renormalized coupling constant u , it indicates the existence of IRFP.

C. improving discretization errors

Since $O(a)$ discretization errors are not improved at all in the lattice actions, it is important to remove the scaling violation as much as possible. To do this, we perform the following improvements on the step scaling function and the DBF before taking the continuum limit.

First let $\sigma(u, s)$ be the continuum limit of $\Sigma_0(u, s, l)$, *i.e.* $\sigma(u, s) = g_{\text{SF}}^2(sL)$ with $u = g_{\text{SF}}^2(L)$. Its perturbative expression is given by

$$\sigma(u, s) = u + s_0 u^2 + s_1 u^3 + s_2 u^4 + \dots, \quad (31)$$

$$s_0 = b_1 \ln(s), \quad (32)$$

$$s_1 = \ln(s) (b_1^2 \ln(s) + b_2), \quad (33)$$

$$s_2 = \ln(s) \left(b_1^3 \ln^2(s) + \frac{5}{2} b_1 b_2 \ln(s) + b_3 \right), \quad (34)$$

where b_i 's are the coefficients of the β -function introduced in sec. II. Recalling the parametric

form of the discretization error [34], the error normalized by $\sigma(u, s)$, denoted by $\delta_0(u, s, l)$, is written as

$$\delta_0(u, s, l) = \frac{\Sigma_0(u, s, l) - \sigma(u, s)}{\sigma(u, s)} = \delta^{(1)}(s, l) u + \delta^{(2)}(s, l) u^2 + O(u^3). \quad (35)$$

With eq. (31), the discretization error at the lowest order in u is found to be

$$\delta^{(1)}(s, l) = \left(p_{1,s \cdot l} - b_1 \ln(s \cdot l) \right) - \left(p_{1,l} - b_1 \ln(l) \right) = p_{1,s \cdot l} - p_{1,l} - b_1 \ln(s). \quad (36)$$

Now by replacing $\Sigma_0(u, s, l)$ in eq. (35) with $\Sigma_1(u, s, l) = \Sigma_0(u, s, l)/(1 + \delta^{(1)}(s, l) u)$, the discretization error reduces to $O(u^2)$. Using $\Sigma_1(u, s, l)$, the one-loop improved DBF is defined by

$$B_1(u, s, l) = \frac{1}{\Sigma_1(u, s, l)} - \frac{1}{u}. \quad (37)$$

This completes the one-loop improvement.

The above procedure can be repeated to an arbitrarily higher order in u , but it requires the perturbative coefficients like $p_{1,l}$ and the perturbative expression of $\sigma(u, s)$ to the corresponding order in u . All the coefficients necessary for the two-loop improvement are not available at this moment. Instead, we follow an alternative prescription proposed in Ref. [37]. After the one-loop improvement, the scaling violation is written as

$$\delta_1(u, s, l) = \frac{\Sigma_1(u, s, l) - \sigma(u, s)}{\sigma(u, s)} = \delta^{(2)}(s, l) u^2 + O(u^3). \quad (38)$$

If one can somehow know $\delta^{(2)}(s, l)$, the scaling violation can be reduced to $O(u^3)$ by replacing $\Sigma_0(u, s, l)$ in eq. (35) with

$$\Sigma_2(u, s, l) = \Sigma_0(u, s, l)/(1 + \delta^{(1)}(s, l) u + \delta^{(2)}(s, l) u^2). \quad (39)$$

$\delta^{(2)}(s, l)$ can be determined by fitting our data for $\delta_1(u, s, l)$ in eq. (38) to the function quadratic in u . Notice that in order for this fitting to make sense, $\sigma(u, s)$ must be known through $O(u^3)$. Since the first two coefficients, b_1 and b_2 , are known, the correct value of $\sigma(u, s)$ can be calculated to $O(u^3)$ as seen from eq. (31).

$\delta_1(u, s, l)$ is fitted to the form of eq. (38), neglecting $O(u^3)$ or higher order terms, for all possible pairs of (s, l) . The fit result is shown in Fig. 2. The fit is performed in a weak coupling region where the perturbative expansion is reliable. Since we have only a limited number of sets of data in such a region, the fit range is extended to $u \sim 2.0$. The

(s, l)	$(4/3, 6)$	$(2, 6)$	$(8/3, 6)$	$(3/2, 8)$	$(2, 8)$	$(4/3, 12)$
$\delta^{(2)}(s, l)$	0.0061(9)	0.0108(13)	0.0131(21)	0.0043(12)	0.0075(21)	0.0034(18)

TABLE VIII: $\delta^{(2)}(s, l)$ for each pair of (s, l) .

extracted values for $\delta^{(2)}(s, l)$ are tabulated in Tab. VIII. As seen from the table, the values of $\delta^{(2)}(s, l)$'s lie between 10^{-2} and 10^{-3} . We can also see that $\delta^{(2)}(4/3, 12)$ is the smallest; this is anticipated because the scaling violation tends to vanish as s approaches to unity or l becomes large. Using $\delta^{(2)}(s, l)$ thus obtained, we define the two-loop improved step scaling function $\Sigma_2(u, s, l)$ in eq. (39), and in turn the two-loop improved DBF

$$B_2(u, s, l) = \frac{1}{\Sigma_2(u, s, l)} - \frac{1}{u}. \quad (40)$$

D. converting the DBF

In the standard analysis, the continuum limit is taken using data sets with a common step scaling factor s and a length scale L , and varying the lattice spacing a ($= L/l$). However, for a given s and L the number of data sets with different a in this work is, at most, two. For example, for $s = 2$ only two data sets, $(s, l) = (2, 6)$ and $(2, 8)$, are available. Although it is still possible to use these two sets of data to take the continuum limit, this causes a problem on the reliability. One possible way to enhance the number of data sets is to interpolate or extrapolate the data of $g_{\text{SF}}^2(g_0^2, l')$ in lattice box size l' to $s \cdot l$. However, a lack of guiding principles in interpolation or extrapolation may cause a systematic uncertainty. In this work, we use an approximate relation to convert the DBF for s into that for s' ($\neq s$) to increase data points used in the continuum extrapolation.

Let us start with a closer look at the discretization error. The discretization error of the lattice DBF, *i.e.* $B_i(u, s, l) - B(u, s)$ ($i=0, 1, 2$), can be expressed in terms of an asymptotic expansion in $1/l$ [34] as

$$B_i(u, s, l) - B(u, s) = \left(\frac{1}{l} - \frac{1}{sl} \right) e_i(u) + O(l^{-2}), \quad (41)$$

where $e_i(u)$ is an unknown coefficient of $O(a)$ error and is a function of u in general. Hereafter higher order terms in $1/l$ are neglected, assuming that they are small. This assumption will

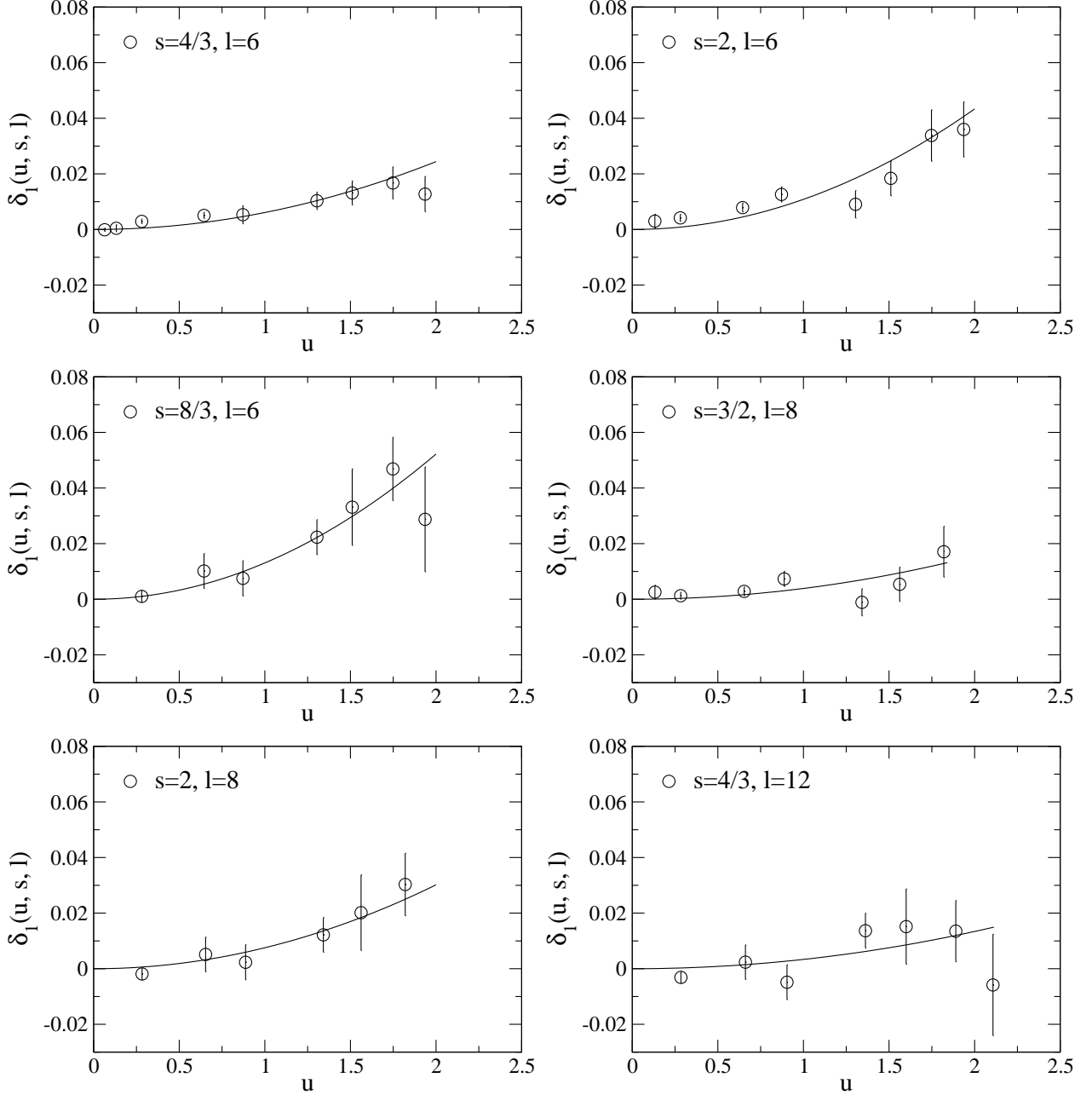


FIG. 2: Fit of δ_1 to a quadratic function of u .

be checked through the scaling behavior later. For the unimproved ($i = 0$), the one-loop improved ($i = 1$) and the two-loop improved ($i = 2$) lattice DBF, the leading order of $e_i(u)$ is $O(u^0)$, $O(u^1)$, $O(u^2)$, respectively.

Here we define the *rescaled* lattice DBF by

$$B'_i(u, s', l, s) = \frac{\ln(s)}{\ln(s')} B_i(u, s', l), \quad (42)$$

and assume, for the continuum DBF, the *key approximation*

$$B(u, s) \approx \frac{\ln(s)}{\ln(s')} B(u, s'). \quad (43)$$

Combining eqs. (41), (42) and (43) together and introducing

$$\xi(s', l, s) = \frac{\ln(s)}{\ln(s')} \left(\frac{1}{l} - \frac{1}{s'l} \right), \quad (44)$$

we arrive at

$$B'_i(u, s', l, s) = B(u, s) + \xi(s', l, s) e_i(u). \quad (45)$$

Since we have six different pairs of (s, l) for the lattice DBF, two unknown coefficients in eq. (45), $B(u, s)$ and $e_i(u)$, for given u and s can be determined by fitting $B'_i(u, s', l, s)$ to a linear function of ξ . Once the continuum DBF, $B(u, s)$, could be determined, the continuum step scaling function, $\sigma(u, s)$, is calculated as

$$\frac{1}{\sigma(u, s)} = \frac{1}{u} + B(u, s). \quad (46)$$

Now let us discuss the validity of the key approximation (43). Solving eq. (1) perturbatively, the continuum DBF is found to be

$$B(u, s) = -\ln(s) \left\{ \frac{\beta(u)}{u^2} + u^2 \ln(s) \frac{1}{2} b_1 b_2 + u^3 \ln(s) \left(\frac{1}{3} b_1^2 b_2 \ln(s) + b_1 b_3 + \frac{1}{2} b_2^2 \right) \right\} + O(u^4 \ln^2(s)). \quad (47)$$

Thus the difference between the r.h.s. and l.h.s in eq. (43) is

$$\begin{aligned} \delta B(u, s, s') &= B(u, s) - \frac{\ln(s)}{\ln(s')} B(u, s') \\ &= u^2 \ln(s) \ln\left(\frac{s}{s'}\right) \left[-\frac{1}{2} b_1 b_2 + u \left\{ -\frac{1}{3} b_1^2 b_2 \ln(ss') - \left(b_1 b_3 + \frac{1}{2} b_2^2 \right) \right\} \right] \\ &\quad + O(u^4 \ln(s) \ln(s/s')). \end{aligned} \quad (48)$$

Since the values of s in our data sets lie between $4/3$ and $8/3$, $\ln(s)$ cannot be larger than unity. Indeed, because of the fact that the numerical values of b_i 's are very small, *e.g.* $b_1 \sim 0.055$, $b_2 \sim -0.002$, $b_3^{\text{SF}} \sim O(10^{-4})$, $\delta B(u, s, s')$ is found to be tiny, at least, in the perturbative regime.

On the other hand, it is difficult to fully check the validity of eq. (43) in the nonperturbative regime. Nevertheless, if the approximation in eq. (43) is sizably violated, the continuum

extrapolation described in the next subsection would not be smooth and hence the large violation may be detectable. Another important point is that if $B(u, s') = 0$ for a certain s' eq. (43) is exact.

In summary, if both of the approximation (43) and the assumption that the $O(a)$ discretization error dominates the others are sizably violated, the linear extrapolation of B' in ξ to the continuum limit would not be smooth. Thus, by monitoring the quality of the continuum extrapolation, the above assumptions can be, at least, partly checked.

E. continuum limit

Figure 3 shows the continuum limit of $B'_i(u, s', l, s)$ ($i=1, 2$) at several representative values of $1/u$, where $s = 2$ is taken. In the preliminary analysis, we have fitted the unimproved (B'_0), the one-loop improved (B'_1) and the two-loop improved (B'_2) DBF separately, and found that all the data are reasonably well described by a linear fit in the region $1/u \gtrsim 0.2$ but in the stronger coupling region ($1/u \lesssim 0.2$) the data points with the largest ξ , *i.e.* the data with $(s, l)=(4/3, 6)$, deviate from the linear line formed by data points with other ξ . A natural explanation is that for this data point $O(a^2)$ or higher order discretization errors are large in the region $1/u \lesssim 0.2$. It was also found that the independent fits of B'_1 and B'_2 give the same continuum limit within statistical error and importantly their values are consistent with the perturbative prediction in the weak coupling region. We therefore decided to make a simultaneous fit of B'_1 and B'_2 to determine the common continuum limit omitting the data with $(s, l)=(4/3, 6)$ which is not shown in the plot. The fit is done for every jack-knife ensemble, and the statistical error in the continuum limit is estimated by the single elimination jack-knife method.

The absolute value of the slope in the linear extrapolation of B'_2 is always equal to or smaller than that of B'_1 , which indicates that the two-loop improvement indeed works. As seen from Fig. 3, in the weak coupling region ($1/u \gtrsim 0.5$), the continuum limit of DBF is clearly negative. This is consistent with the asymptotic freedom and means that the effective coupling constant grows with its length scale in this region. In contrast, in the strong coupling region ($1/u \lesssim 0.15$) the continuum limit is clearly positive, *i.e.* the sign of the DBF is flipped somewhere in $0.15 < 1/u < 0.5$. This suggests the existence of the infrared fixed point. In order to determine the precise value of the fixed point we need more

statistics, but the sign flip of the DBF is already clear enough.

As stated already, the rescaled lattice DBF's well align independently of s' , and the deviation is not clear within the statistical uncertainty. This supports that the assumptions of eq. (43) and the linear scaling violation are valid within the size of the uncertainty. Notice that the data sets contain the data with $(s, l)=(2, 6)$ (rightmost data) and $(2, 8)$ (second from the left). We can estimate the continuum limit using these two points by only assuming the linear dependence but without the approximation (43). The continuum limits thus obtained turn out to be consistent with those in Fig. 3 within statistical uncertainty, and importantly the sign-flip is found to persist. This observation gives another support to the assumption we made.

The sign-flip of the DBF is further checked by using the data obtained at $\beta = 4.55$ ($g_0^2 \approx 1.32$) on the $l = 18$ lattice. Since the data with $l = 18$ is available only at $\beta = 4.55$, the two-loop improvement through the fit to eq. (38) is not possible and hence only the one-loop improved DBF is discussed below. However, recalling that $\delta^{(2)}(s, l)$ tends to vanish as s approaches to unity or l becomes large, $\delta^{(2)}(9/8, 16)$ is expected to be smaller than $\delta^{(2)}(4/3, 12)$ and hence be negligible. We construct the one-loop improved lattice DBF with $(s, l)=(9/8, 16)$ at $\beta = 4.55$ with $1/u = 1/g_{\text{SF}}^2(1.32, 16) = 0.0884$ and then rescale it by multiplying $(\ln(2)/\ln(9/8))$. The continuum extrapolation at $1/u = 0.0884$ is shown in Fig. 4, where the data point thus obtained (filled circle) is overlaid on the results from the other lattices (open symbols). While the fit lines are obtained with the open symbols only, it is right on the top of them. This confirms that at such a large coupling constant the DBF is positive.

Figure 5 shows the $1/u$ dependence of the continuum DBF, where the results are compared with the perturbative results. It is seen that the nonperturbative DBF roughly follows the perturbative ones down to $1/u \sim 0.5$. Then the running slows down, *i.e.* walks, and eventually the coupling constant reaches a fixed point at $0.2 \lesssim 1/u \lesssim 0.3$. The scale dependence of the inverse of the SF coupling constant is plotted in Fig. 6, where the perturbative predictions are also shown for comparison.

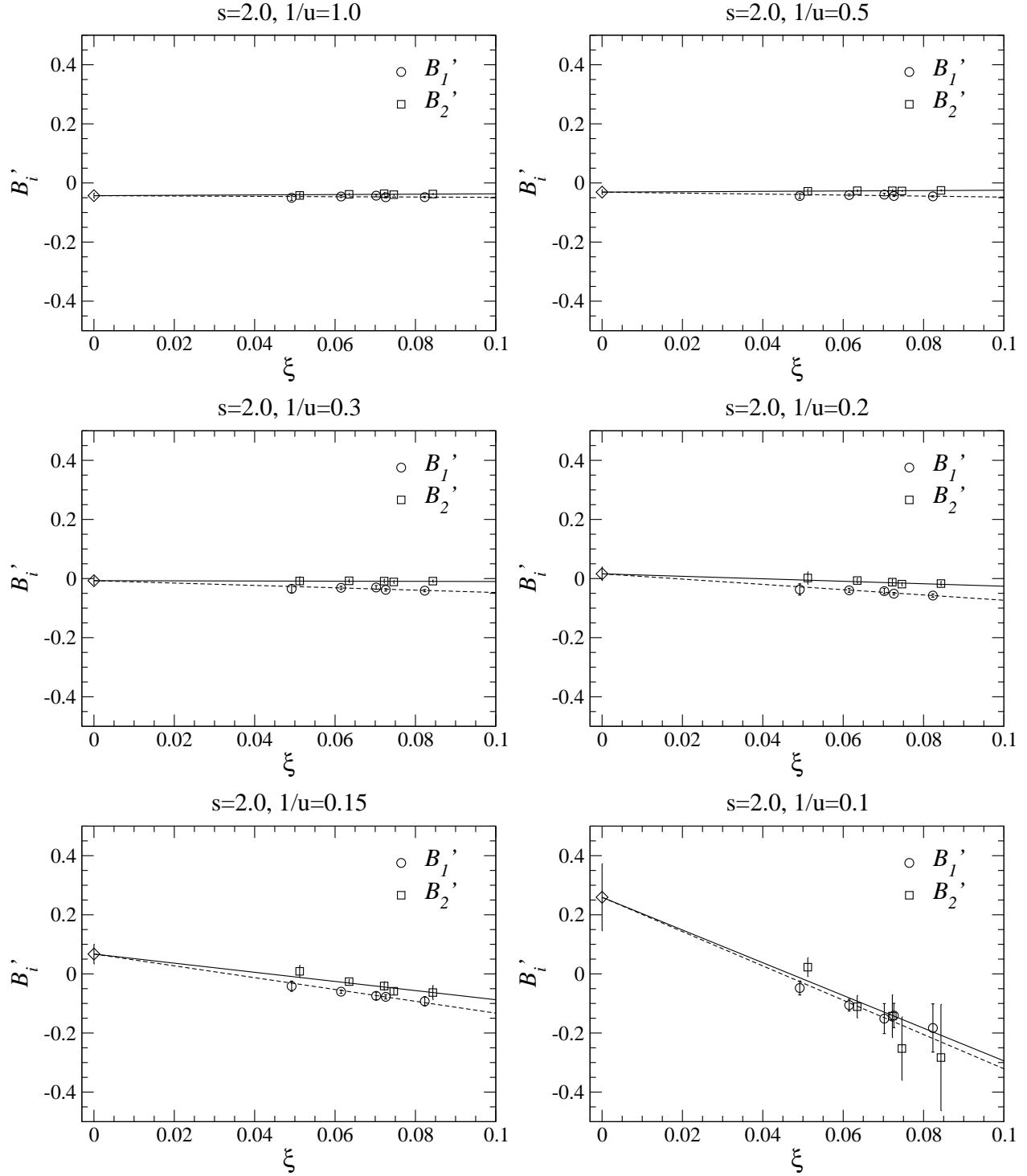


FIG. 3: Simultaneous fit of B'_1 (circles) and B'_2 (squares) to the continuum limit (diamonds) using eq. (43). The data points are slightly shifted in horizontal direction for clarity. The values of (s', l) of each data are $(2, 6)$, $(8/3, 6)$, $(3/2, 8)$, $(2, 8)$, and $(4/3, 12)$ from right to left.

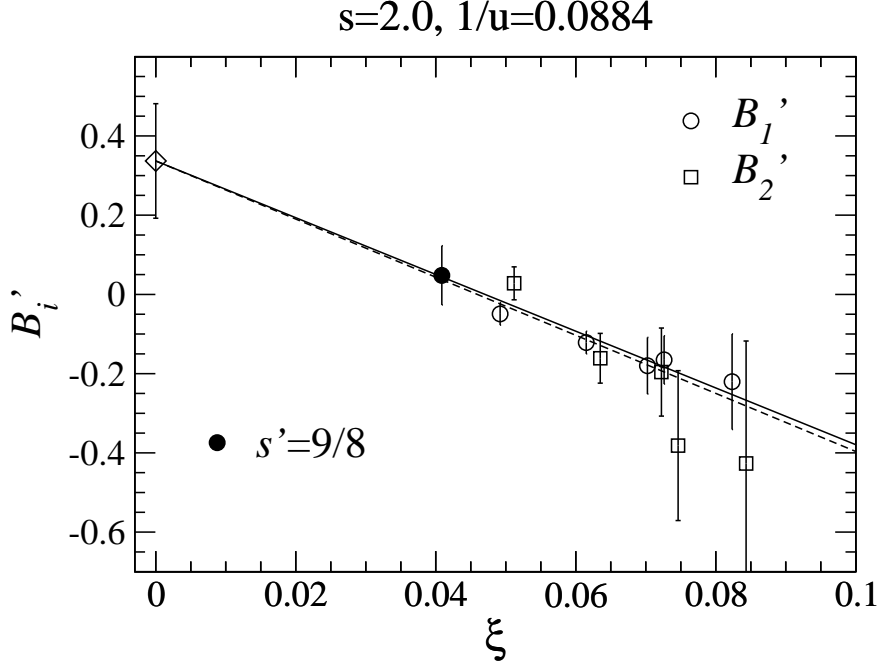


FIG. 4: Same as Fig. 3 but the data point obtained with $(s', l)=(9/8, 16)$ (filled circle) is overlaid at $s = 2.0$ and $1/u=0.0884$.

V. SUMMARY AND OUTLOOK

In this work, the running coupling constant of ten-flavor QCD is numerically investigated using lattice technique. The continuum limit of the DBF is taken linearly assuming that the $O(a)$ discretization error dominates the others. The result shows the sign-flip of the DBF at the inverse of the gauge coupling constant, $0.2 \lesssim 1/u \lesssim 0.3$, or equivalently $3.3 \lesssim g_{\text{SF}}^2(L) \lesssim 5$. The data with the largest lattice size ($l = 18$) in this work supports the existence of the infrared fixed point. In order to determine the precise value of the fixed point, more statistics and data from larger lattices are necessary. Combining with the results of Ref. [12], the critical number of flavors which separates the conformal and the broken phases is estimated to be in the region of $8 < N_f^{\text{crit}} < 10$.

As mentioned in sec. I, the conformal window could be studied by looking at spectroscopy or renormalization group analysis on the lattice or with models. The conclusions based on various methods are not consistent among them. In order to pin down N_f^{crit} , these contradictions must be clarified with further studies.

What is really important in the context of the WTC is the anomalous dimension of the $\bar{\psi}\psi$ operator. The calculation of the anomalous dimension in ten-flavor QCD is on-going.

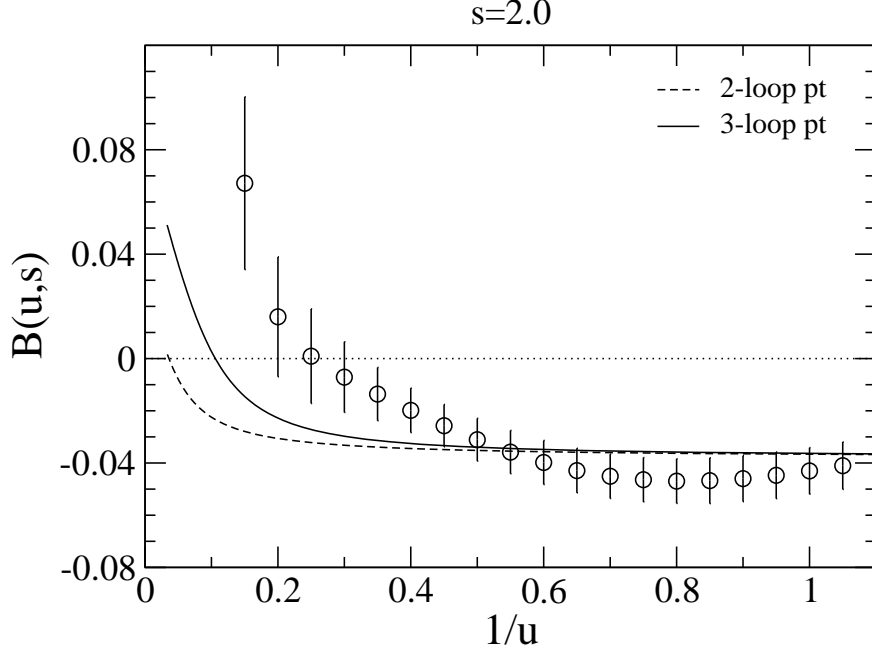


FIG. 5: $1/u$ dependence of $B(u, s)$ with $s=2$ obtained from the simultaneous linear fit.

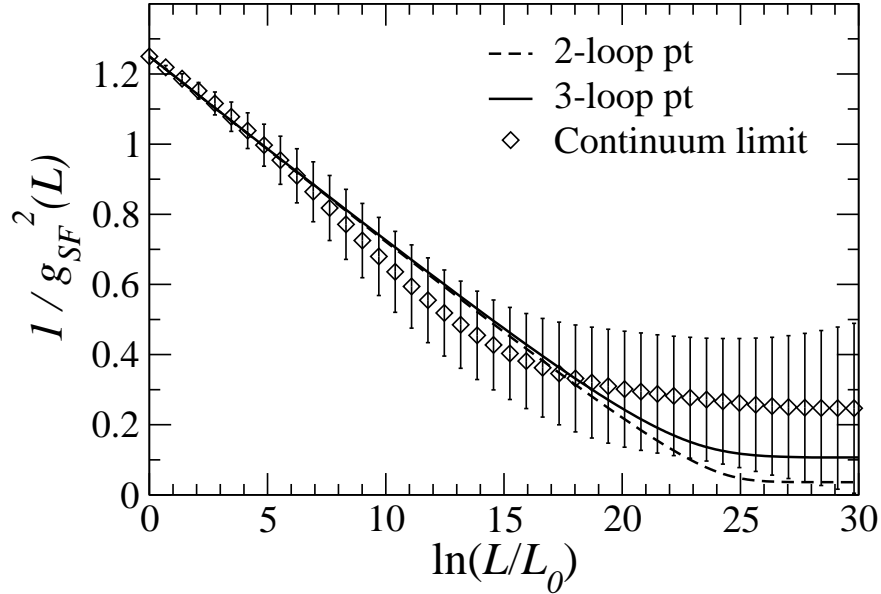


FIG. 6: The running coupling in the continuum limit is compared with the perturbation.

The result will be published elsewhere.

Once one has fixed an attractive candidate for WTC, the next important step would be the calculation of the S -parameter. The calculational method has been established in Ref. [38], where the QCD S -parameter is calculated on the lattice for the first time and is correctly reproduced. Later, the method was applied to three-flavor QCD [39], sextet QCD [40] and

six-flavor QCD [41]. In Ref. [41], the evidence of the reduction of S -parameter is reported. Another important quantity which should be calculated is obviously the mass spectrum of the candidate theory, including vector and scalar resonances, the decay constant of the NG boson and the chiral condensate. Although the precise determinations of these quantities are challenging, the direct comparison with the upcoming LHC results is extremely interesting and hence we believe that such calculations are worth a lot of efforts.

VI. ACKNOWLEDGMENT

N.Y. thanks the Aspen Center for Physics where the workshop “Strong Coupling Beyond the Standard Model” were held during May and June 2010 and the Yukawa Institute for Theoretical Physics at Kyoto University for supporting the YITP workshop “Summer Institute 2010” (YITP-W-10-07). N.Y. would also like to thank Hideo Matsufuru, Yoshio Kikukawa and Takashi Kaneko for useful discussion. A part of this work was completed during these workshops. The main part of the numerical simulations were performed on Hitachi SR11000 and the IBM System Blue Gene Solution at High Energy Accelerator Research Organization (KEK) under a support of its Large Scale Simulation Program (No. 09/10-01, 10-15), on B-factory computer system at KEK, on GCOE (Quest for Fundamental Principles in the Universe) cluster system at Nagoya University, and on the INSAM (Institute for Numerical Simulations and Applied Mathematics) GPU cluster at Hiroshima University. This work is supported in part by the Grant-in-Aid for Scientific Research of the Japanese Ministry of Education, Culture, Sports, Science and Technology (Nos. 20105001, 20105002, 20105005, 21684013, 22740183, 22011012, 20540261, 22224003, 20740139, 18104005, 22244018, and 227180), and by US DOE grant #DE-FG02-92ER40699.

-
- [1] S. Weinberg, Phys. Rev. D **13**, 974 (1976); L. Susskind, Phys. Rev. D **20**, 2619 (1979);
 - [2] E. Eichten and K. D. Lane, Phys. Lett. B **90**, 125 (1980); S. Dimopoulos and L. Susskind, Nucl. Phys. B **155**, 237 (1979).
 - [3] R. S. Chivukula, arXiv:hep-ph/0011264; C. T. Hill and E. H. Simmons, Phys. Rept. **381**, 235 (2003) [Erratum-ibid. **390**, 553 (2004)] [arXiv:hep-ph/0203079]; F. Sannino, arXiv:0804.0182 [hep-ph].

- [4] M. E. Peskin and T. Takeuchi, Phys. Rev. Lett. **65**, 964 (1990); Phys. Rev. D **46**, 381 (1992).
- [5] See, for example, R. S. Chivukula and E. H. Simmons, Phys. Rev. D **82**, 033014 (2010) [arXiv:1005.5727 [hep-lat]].
- [6] B. Holdom, Phys. Rev. D **24**, 1441 (1981); K. Yamawaki, M. Bando and K. i. Matumoto, Phys. Rev. Lett. **56**, 1335 (1986); T. W. Appelquist, D. Karabali and L. C. R. Wijewardhana, Phys. Rev. Lett. **57**, 957 (1986); T. Akiba and T. Yanagida, Phys. Lett. B **169**, 432 (1986); M. Bando, T. Morozumi, H. So and K. Yamawaki, Phys. Rev. Lett. **59**, 389 (1987).
- [7] D. D. Dietrich and F. Sannino, Phys. Rev. D **75**, 085018 (2007) [arXiv:hep-ph/0611341].
- [8] W. E. Caswell, Phys. Rev. Lett. **33**, 244 (1974); T. Banks and A. Zaks, Nucl. Phys. B **196**, 189 (1982).
- [9] For recent review, see, for example, G. T. Fleming, PoS **LATTICE2008**, 021 (2008) [arXiv:0812.2035 [hep-lat]]; E. Pallante, arXiv:0912.5188 [hep-lat];
- [10] H. Gies and J. Jaeckel, Eur. Phys. J. C **46**, 433 (2006) [arXiv:hep-ph/0507171].
- [11] J. Braun and H. Gies, JHEP **0606**, 024 (2006) [arXiv:hep-ph/0602226].
- [12] T. Appelquist, G. T. Fleming and E. T. Neil, Phys. Rev. Lett. **100**, 171607 (2008); [arXiv:0712.0609 [hep-ph]]; Phys. Rev. D **79**, 076010 (2009). [arXiv:0901.3766 [hep-ph]].
- [13] A. Deuzeman, M. P. Lombardo and E. Pallante, Phys. Lett. B **670**, 41 (2008) [arXiv:0804.2905 [hep-lat]].
- [14] A. Deuzeman, M. P. Lombardo and E. Pallante, Phys. Rev. D **82**, 074503 (2010) [arXiv:0904.4662 [hep-ph]].
- [15] Z. Fodor, K. Holland, J. Kuti, D. Nogradi and C. Schroeder, Phys. Lett. B **681**, 353 (2009) [arXiv:0907.4562 [hep-lat]].
- [16] A. Hasenfratz, Phys. Rev. D **80**, 034505 (2009) [arXiv:0907.0919 [hep-lat]].
- [17] X. Y. Jin and R. D. Mawhinney, arXiv:0910.3216 [hep-lat].
- [18] E. Bilgici *et al.*, arXiv:0910.4196 [hep-lat].
- [19] Y. Shamir, B. Svetitsky and T. DeGrand, Phys. Rev. D **78**, 031502 (2008) [arXiv:0803.1707 [hep-lat]].
- [20] T. DeGrand, Y. Shamir and B. Svetitsky, Phys. Rev. D **79**, 034501 (2009) [arXiv:0812.1427 [hep-lat]].
- [21] T. DeGrand, Phys. Rev. D **80**, 114507 (2009) [arXiv:0910.3072 [hep-lat]].
- [22] T. DeGrand, Y. Shamir and B. Svetitsky, arXiv:1006.0707 [hep-lat].

- [23] Z. Fodor, K. Holland, J. Kuti, D. Nogradi and C. Schroeder, JHEP **0911**, 103 (2009) [arXiv:0908.2466 [hep-lat]].
- [24] J. B. Kogut and D. K. Sinclair, Phys. Rev. D **81**, 114507 (2010) [arXiv:1002.2988 [hep-lat]].
- [25] A. J. Hietanen, K. Rummukainen and K. Tuominen, Phys. Rev. D **80**, 094504 (2009) [arXiv:0904.0864 [hep-lat]].
- [26] A. J. Hietanen, J. Rantaharju, K. Rummukainen and K. Tuominen, JHEP **0905**, 025 (2009) [arXiv:0812.1467 [hep-lat]].
- [27] L. Del Debbio, B. Lucini, A. Patella, C. Pica and A. Rago, Phys. Rev. D **80**, 074507 (2009) [arXiv:0907.3896 [hep-lat]].
- [28] F. Bursa, L. Del Debbio, L. Keegan, C. Pica and T. Pickup, Phys. Rev. D **81**, 014505 (2010) [arXiv:0910.4535 [hep-ph]].
- [29] L. Del Debbio, B. Lucini, A. Patella, C. Pica and A. Rago, Phys. Rev. D **82**, 014509 (2010) [arXiv:1004.3197 [hep-lat]].
- [30] L. Del Debbio, B. Lucini, A. Patella, C. Pica and A. Rago, Phys. Rev. D **82**, 014510 (2010) [arXiv:1004.3206 [hep-lat]].
- [31] M. Luscher, R. Narayanan, P. Weisz and U. Wolff, Nucl. Phys. B **384** (1992) 168 [arXiv:hep-lat/9207009]; M. Luscher, R. Sommer, P. Weisz and U. Wolff, Nucl. Phys. B **413**, 481 (1994) [arXiv:hep-lat/9309005]; S. Sint and R. Sommer, Nucl. Phys. B **465**, 71 (1996) [arXiv:hep-lat/9508012].
- [32] S. Aoki *et al.* [JLQCD Collaboration], Phys. Rev. D **72**, 054510 (2005) [arXiv:hep-lat/0409016].
- [33] K. i. Nagai, G. Carrillo-Ruiz, G. Koleva and R. Lewis, Phys. Rev. D **80**, 074508 (2009) [arXiv:0908.0166 [hep-lat]].
- [34] A. Bode, P. Weisz and U. Wolff [ALPHA collaboration], Nucl. Phys. B **576**, 517 (2000) [Erratum-ibid. B **600**, 453 (2001 ERRAT,B608,481.2001)] [arXiv:hep-lat/9911018].
- [35] T. Appelquist, K. D. Lane and U. Mahanta, Phys. Rev. Lett. **61**, 1553 (1988); A. G. Cohen and H. Georgi, Nucl. Phys. B **314**, 7 (1989).
- [36] M. Hayakawa, K.-I. Ishikawa, Y. Osaki, S. Takeda, S. Uno, N. Yamada, arXiv:1009.5169 [hep-lat].
- [37] S. Aoki *et al.* [PACS-CS Collaboration], JHEP **0910**, 053 (2009) [arXiv:0906.3906 [hep-lat]].
- [38] E. Shintani *et al.* [JLQCD Collaboration], Phys. Rev. Lett. **101**, 242001 (2008)

[arXiv:0806.4222 [hep-lat]].

[39] P. A. Boyle, L. Del Debbio, J. Wennekers and J. M. Zanotti [RBC Collaborations and UKQCD Collaborations], Phys. Rev. D **81**, 014504 (2010) [arXiv:0909.4931 [hep-lat]].

[40] T. DeGrand, arXiv:1006.3777 [hep-lat].

[41] T. Appelquist *et al.*, arXiv:1009.5967 [hep-ph].